FEBS Letters 587 (2013) 3709–3714

FEBS Letters

journal homepage: www.FEBSLetters.org

Remaining structures at the N- and C-terminal regions of alpha-synuclein accurately elucidated by amide-proton exchange NMR with fitting

Honoka Okazaki [a], Yuka Ohori [a], Masaya Komoto [a], Young-Ho Lee [b], Yuji Goto [b], Naoya Tochio [c], Chiaki Nishimura [a,b,*]

[a] Faculty of Pharmaceutical Sciences, Teikyo Heisei University, Nakano, Tokyo 164-8530, Japan
[b] Institute for Protein Research, Osaka University, Suita, Osaka 565-0871, Japan
[c] NMR Facility, Center for Life Science Technologies, Yokohama Institute, RIKEN, Yokohama, Kanagawa 230-0045, Japan

ARTICLE INFO

Article history:
Received 17 June 2013
Revised 26 August 2013
Accepted 25 September 2013
Available online 7 October 2013

Edited by Christian Griesinger

Keywords:
Alpha-synuclein
Unfolded protein
NMR
Protein folding
Amide proton exchange

ABSTRACT

Alpha-synuclein is analyzed in physiological conditions by CLEANEX-PM methodology, in which the amide-proton exchange can be monitored at millisecond scale. The relationship between k_{ex} and $[OH]^-$ is confirmed as a linear correlation with slope 1, indicating EX2 regime. There are significant residual structures at the N- and C-terminal regions. The structure at the C-terminal region is more stable than that of the N-terminal region. The middle part including NAC region is not completely protected. The data acquired at various pH and mixing time conditions followed by linear fitting give accurate information about residual structures.

1. Introduction

Parkinson disease (PD) is caused by the conversion of the soluble alpha-synuclein [1] protein to the insoluble oligomer and fibril in the Lewy bodies [2]. The analysis of the formation of the insoluble species of alpha-synuclein is really important to rescue the patient with PD [3]. The information about the structure of the soluble form is used to develop the new drug.

The advantage using NMR is to enable us to analyze the solution dynamical structure of the protein. Generally, the dynamical structure has been analyzed by using many different NMR techniques, including paramagnetic relaxation enhancement (PRE) [4], residual dipolar coupling (RDC) [5], and R_2 relaxation dispersion experiments [6]. The intrinsically disordered protein has only limited structure by itself in the physiological condition, and the rigid structure can be formed upon binding to the other protein in some cases [6]. The human alpha-synuclein has only the limited and residual structure in a monomer at the neutral pH [7]. However, this structure might be a key structure related to the core formation of the amyloid fibril. The consensus idea based on the experiments with the soluble and monomeric alpha-synuclein is that either N-terminal or C-terminal, or both regions prevent the amyloid formation by forming the long-range interaction [8]. The middle domains (non-A-beta-amyloid component (NAC) region) [9] in each molecule take the beta-structure and are interacted each other inter-molecularly in the fibril [10].

The hydrogen/deuterium (HD) exchange is very powerful strategy for the estimate of the formation of the hydrogen bond as well as the ratio of the area buried [11]. However, there are some limitations for the actual experiments of the unfolded proteins: (1) the reaction of the HD exchange is done so quickly compared to the time duration for the data acquisition that it is difficult to distinguish between the completely unfolded and remaining structural regions in case of the intrinsically disordered protein. (2) It is the time-consuming step to start the HD exchange reaction either by the addition of the deuterium buffer to the lyophilized powder of protein, or by the buffer change with the gel filtration column.

On the other hand, in case of the clean chemical exchange-phase modulated (CLEANEX-PM) experiment we just need to prepare the regular NMR sample [12–14]: namely, the deuterium buffer for the initiation of the exchange between bulk water proton

* Corresponding author. Address: 4-21-2 Nakano, Nakano-ku, Tokyo 164-8530, Japan.
E-mail address: cnishimura@thu.ac.jp (C. Nishimura).

0014-5793/$36.00
http://dx.doi.org/10.1016/j.febslet.2013.09.039

and amide proton in protein is not required. The CLEANEX-PM experiment, which enables us to have many different data points, is more suitable to estimate the differences of the weak protection between the residual structure and completely unfolded structure. Here, the CLEANEX-PM data has been acquired at the various pH and mixing time conditions followed by the linear fittings to get detail information about the residual structure.

2. Materials and methods

2.1. Protein preparation

Recombinant human alpha-synuclein was expressed by the cell-free expression system in RIKEN. The ^{15}N-labeled and ^{15}N, ^{13}C double-labeled protein were produced and purified by the affinity and ion-exchange columns. All NMR samples were dissolved in the deuterated 20 mM Tris–HCl buffer with 100 mM NaCl and 10% D_2O at the various pHs. The Centriprep 10 cartridge (Amicon) was used for the buffer change prior to the NMR experiments.

2.2. NMR spectroscopy

Backbone resonance assignments of the alpha-synuclein at pH 7 and 15 °C were made using 3D HNCO, HNCACO, HNCA, and HNCOCA [15]. 3D HNCACB were also collected for the determination of the amino acid type. The CLEANEX-PM experiments were performed at 15 °C, at various pH and exchange duration times. The CLEANEX-PM transverse relaxation optimized spectroscopy (TROSY) heteronuclear single quantum coherence (HSQC) experiments [13] were performed with mixing times (0.005, 0.010, 0.015, 0.02, 0.05, 0.1 s). Spectra were collected with an increment delay of 3 s. As a reference, TROSY HSQC without the mixing times was collected. All spectra were recorded on Bruker Avance 600 spectrometer equipped with a triple-resonance CryoProbe and processed using NMRPipe [16].

3. Results

3.1. Two different strategies of the process of the exchange of amide-proton

Fig. 1A shows the ratio of the exchange of each amide-proton in the amino-acid sequence during the different duration time. As expected, the longer incubation time (100 ms) allowed more exchange between the water proton and amide proton than the shorter time (20 ms). At a glance, the residues at the C-terminal region between the 100 and 140 show the less ratio of the exchange compared to the other region.

We processed the data in two different manners from here. In one process, the k_{ex} values of each residue at the different pHs were calculated first, and then the calculation of the extrapolated values ($A0$) of the k_{ex} based on the different pH data was performed (Figs. 1 and 2). In another process, first the midpoint of the sigmoid curve was calculated based on the transition of the exchange ratio of each residue as a function of pH, and then the calculation of the extrapolated midpoint values ($B0$) of the transition was performed with the different duration times (Figs. 3 and 4B).

3.2. k_{ex} and A0

Fig. 1B shows the transition of the ratio of the exchange during the various incubation times including 5, 10, 15, 20, 50, and 100 ms at pH 7. The exponential fittings were performed with the kinetic data at each residue.

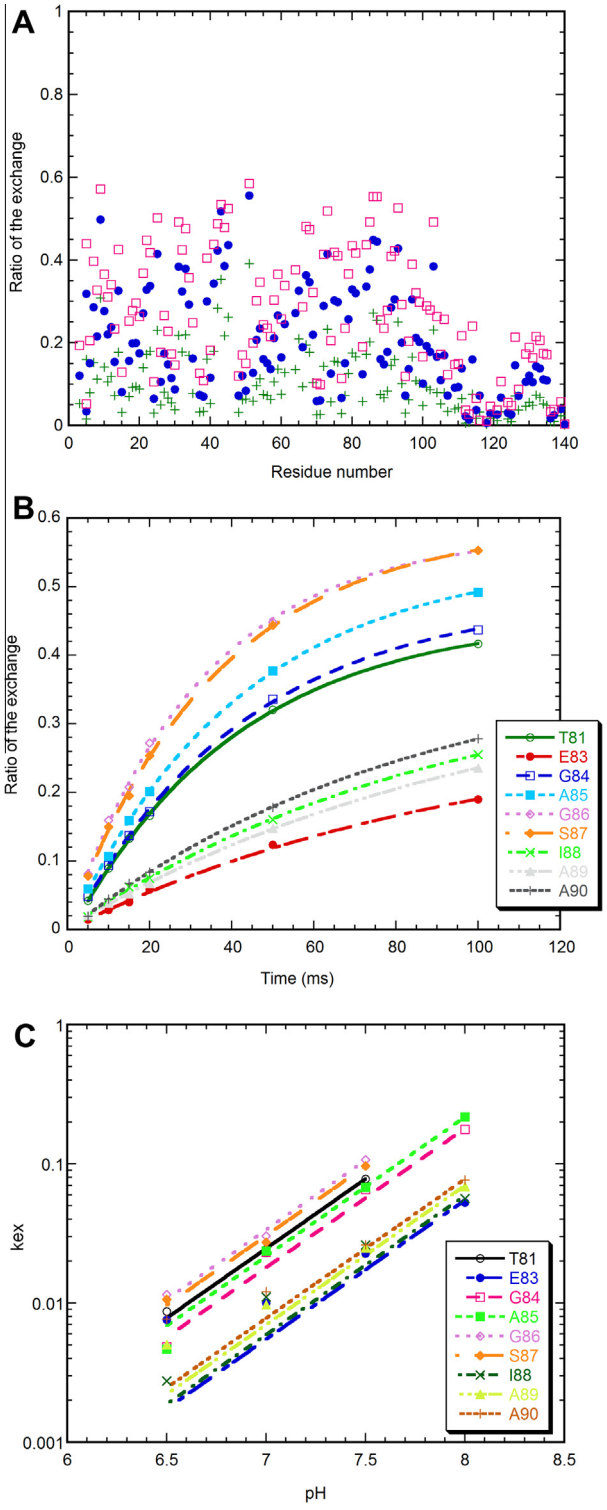

Fig. 1. (A) The ratio of the proton exchange between the amide in protein and bulk water during the different duration (20 ms (+), 50 ms (●), and 100 ms (□)) monitored by the CLEANEX-PM experiments. (B) The exponential fitting to the ratio of the kinetic exchange of the each residue at T81–A90. (C) The linear fitting to the relationship between the solution pH and k_{ex}. The k_{ex} values were calculated based on the exponential fitting in Fig. 1B.

Fig. 1C reveals that the data of the k_{ex} values of each amino-acid at the four different pHs (6.5, 7.0, 7.5, and 8.0) are fitted by the formula (1) shown below.

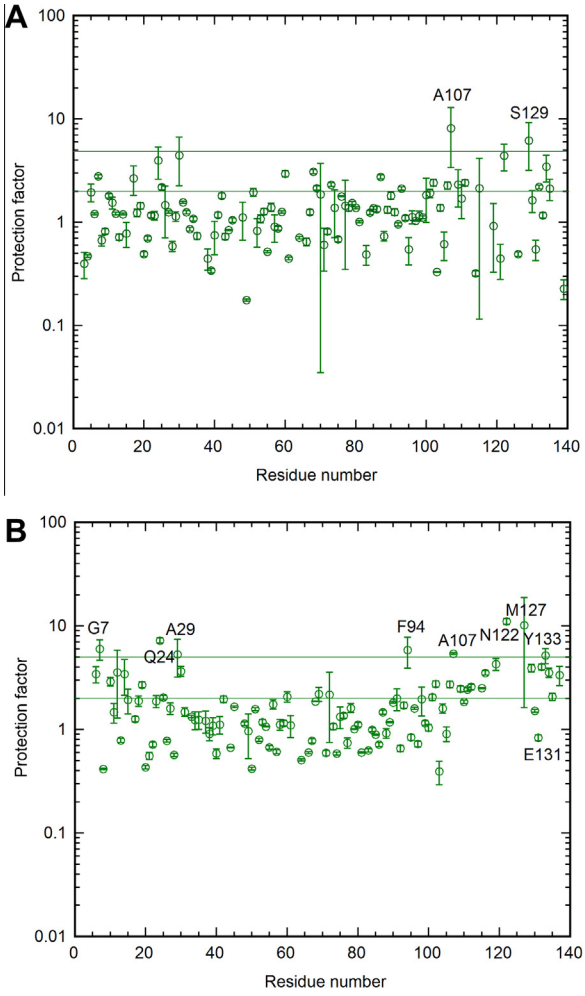

Fig. 2. The protection factors as a function of the residue number. The values of the kinetic constants were normalized using the intrinsic exchange rate of each amino-acid in the sequence. (A) The protection factors calculated based on one data set at pH 7.0. (B) The protection factors based on the calculated value (*A*0). Four data sets were used for the linear fitting as shown in Fig. 1C in order to calculate the *A*0. The residue numbers are shown whose values of the protection factor are more than five and E131. Error bars are included.

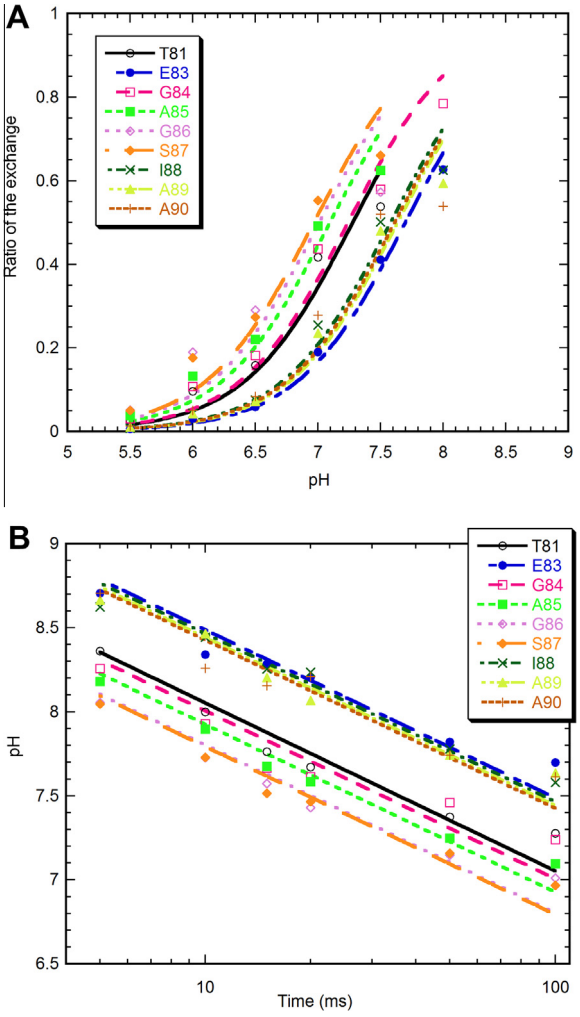

Fig. 3. (A) The relationship between the solution pH and exchange ratio. The Henderson–Hasselbalch equation [32] was used for the fitting of the sigmoid curves. (B) The midpoints of the transition of the exchange ratio for each residue were calculated in Fig. 3A, and plotted in Fig. 3B as a function of the time duration for the exchange. The linear fittings were performed between the time duration and midpoint, and the *B*0 values were calculated.

$$Y = A0 * (10^{(X)}) \quad (1)$$

The linear fitting indicated the rate constant (k_{ex}) is 1:1 proportional to [OH^-] with the slope 1 [14]. Our experimental data from CLEANEX-PM was confirmed to be in the EX2 regime. Secondly, we calculated the extrapolated values (*A*0) based on the fitting, which is the value at pH 0. Finally, the protection factor was calculated using the intrinsic exchange rate [17] to normalize the each *A*0 value of the different type of amino-acid.

3.3. Protection factor derived from k_{ex} at pH 7

Fig. 2A represents the calculated result of the protection factors only using the data at pH 7.0. Namely, it was calculated only based on the kex values in Fig. 1B. The most values are near one, which shows no protection. However, some errors are not negligible in this figure, and it is somehow difficult to conclude which region has the protection or not.

3.4. Protection factor from A0

On the other hand, the Fig. 2B data is more informational and convincing, in which the three extra data points at pH 6.5, 7.5, and 8.0 are included in addition to those at pH 7.0, and the *A*0 value for the protection calculation was acquired after the linear fitting (Fig. 1C). The residues at the N-terminal region including G7, Q24, and A29 can be more protected than the others. In addition, the residues at the C-terminal region including the F94, A107, N122, M127, and Y133 are significantly more protected.

3.5. Midpoint of the transition of the pH and B0 (second strategy)

For the second strategy, the Fig. 3A was shown as the example of the pH dependency on the exchange ratio regarding T81–A90. As expected, the relationship between two parameters (pH and exchange ratio) indicates the sigmoid-curve [18]. Fig. 3A is the 100 ms-exchange experiment by CLEANEX-PM at the different pHs including 5.5, 6.0, 6.5, 7.0, 7.5, and 8.0. When the reaction is faster, the reaction curve shifts to the left side. Therefore, the midpoint of the transition in the sigmoid curve can be another probe for the estimation of the reaction kinetics (Fig. 3A).

Next, Fig. 3B indicates the relationship between the exchange mixing time and the midpoint of the transition of pH. The data at six different durations including 5, 10, 15, 20, 50, and 100 ms were plotted against the calculated midpoint values of the transition.

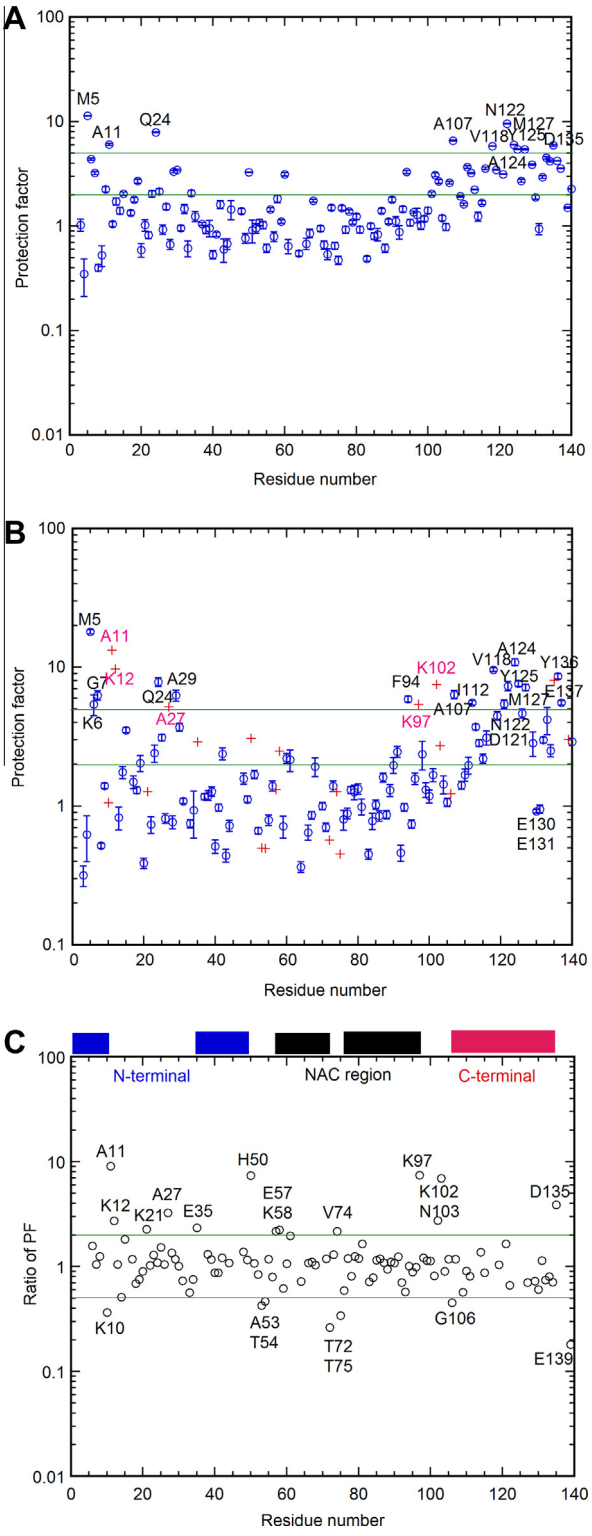

Fig. 4. (A) The protection factors calculated by one data set at 100-ms duration, and (B) the factors calculated by the *B0* values based on the six data sets at 5, 10, 15, 20, 50, and 100 ms duration. The residue numbers, whose protection factors are more than five and E130 and E131, were shown. Two types of plots (○) and (+) are used. The data (open circle) points are reliable, whose values are almost identical between the Figs. 2B and 4B with the different calculations as shown below. Error bars are indicated. (C) The difference of the data by the different calculation strategies. The ratios of the protection factors (Fig. 4B/2B) were shown. The residues, whose values are more than two or less than 0.5, are shown as the residue numbers, and shown as (+) in Fig. 4B. The regions, where two strategies give the consistent values, are shown by the bars on the top of the figure.

The linear relationship of the duration time for the exchange was confirmed against the midpoint of the pH transition as shown in an Eq. (2).

$$Y = B0 - \log(X) \tag{2}$$

The extrapolated value of the midpoint of pH from the different mixing times, which we call as *B0* (mixing time vs. pH midpoint) at 1 ms, is a similar parameter to the *A0* (pH vs. kex) (Fig. 3B). But, the pH in Fig. 1C is inversely proportional to the pH midpoint in Fig. 3A and B. Therefore, it was shown that the duration time and [OH^-] have a linier relationship with the slope-1 (Fig. 3B). The values of the midpoints were fitted to be inversely proportional to the duration time, indicating the EX2 regime, again. The intrinsic exchange ratio was used for the further calculation of the protection factor [18] (Fig. 4A and B).

In this case, the $t_{1/2}$ (time for the half-reaction) is calculated from the intrinsic exchange rate ($k_{ex,int}$) at pH 7 for example. Next, the $pH_{1/2,int}$, which needs the half reaction of the unprotected proton for 1 ms duration, can be calculated by the formula (3) as shown below.

$$10^{(7-pH_{1/2,int})} = 1/t_{1/2,pH7} \tag{3}$$

The protection factor (PF) is calculated with the formula (4).

$$PF = 10^{((pH_{1/2,obs})/pH_{1/2,int})} \tag{4}$$

where the $pH_{1/2,obs}$ is *B0*.

For instance, the expected curves for unprotected amides are shown as a function of pHs in the paper [18]. In case of 100-ms duration, the $pH_{1/2,int}$ for 100 ms was calculated.

3.6. Protection factor from the midpoint of pH at 100 ms

Fig. 4A reveals the protection factor as a function of the residue number in case of only 100 ms exchange duration. This calculation was done based on the midpoint of the pH transition using only Fig. 3A data. The residues at both N-terminus and particularly C-terminal region seem to be more protected than the others. Interestingly, there are three different types of residues at the N-terminal domain: some residues are significantly more protected (M5, A11, and Q24) than others. The other residues seem to be not protected at all, and take the random coil structure even at the same region based on the protection factor data. However, the C-terminal residues at 120–140 seem to be significantly more protected than the residues in any other regions. Particularly, the residues (A107, V118, N122, A124, Y125, M127, and D135) indicate higher protection, whose protection factors are more than five. The data in Fig. 4A is basically similar to those of Fig. 2B. However, the data in Fig. 4A is much clearer to show the remaining structure especially at the C-terminal region.

3.7. Protection factor from B0

Fig. 4B shows the protection factors based on the calculated *B0* values from the Fig. 3B. Fig. 4B seems to be similar to the Fig. 4A. But additionally some residues are more significantly protected (K6, G7, K12, A27, and A29) at the N-terminal region, and (F94, K97, A102, I112, D121, Y136, and E137) at the C-terminal region in Fig. 4B. Interestingly, as seen in Fig. 4A, most of all C-terminal residues (A107–A140) have the higher protection factors corresponding to the stable residual structure rather than the random coil structure. Only E130 and E131 are somewhat less protected compared with the other C-terminal residues. On the other hand, at the N-terminal region, some residues have the higher protection factors, whereas the others have the lower values. By contrast, all residues at the NAC region (K60–V95) are monotonously less

protected than the residues in the other regions including the N- and C- terminal regions. The residues at A30–T59 are also not protected at all.

4. Discussion

4.1. Advantage of the data collection at different pHs

For the analysis of the remaining structure of α-synuclein, the data of CLEANEX-PM was collected at different pHs and exchange durations. There are two benefits for collecting data at different pHs: (1) the EX2 regime can be confirmed as a function of pH [14], and (2) the second strategy (Sections 3.5–3.7) using the midpoint of pH transition can be also employed including the calculation of *B*0. Namely, the different processes can be tested and compared using the data at different pHs as shown below.

However, it is not clear why the extrapolation results gave the better data (Fig. 2A and B). It is probably simply due to the better statistics with four data sets instead of one data set.

4.2. Comparison of two data derived from the different processes

To check the reliability of the data (Fig. 4C), the protection factors in Fig. 4B were divided by the protection factors in Fig. 2B. The ratio at all residues should be close to one. It is because the data are identical, but two procedures of calculations are different. The ratios regarding some residues were not close to one, indicating significant errors included in the calculations. In Fig. 4C, the residues, whose ratio is more two or less 0.5, have been shown as the residue numbers. Interestingly, the border region between the N-terminal and NAC domains (H50, A53, T54, E57, and K58) and another border region between the NAC and the C-terminal (K97, K102, N103, and G106) domains give the different values between two procedures. The residues at the C-terminal region including D135 and E139 also indicate the different values. Namely, these significant errors in the calculations seem to be observed specific to the border area, probably because the protection factor can be more sensitive to the change of the environments especially at the border area. In addition, T72, V74, and T75, which are located in the middle of the NAC region, show the different tendency between two calculated values. Interestingly, K10, A11, K12, K21, A27 and E35 also indicate the large differences, which are located in the N-terminal domain.

4.3. EX2 and EX1 regimes

We also had checked the EX2 regime [19] in the CLEANEX-PM experiments to monitor the exchange kinetics as functions of the pHs and mixing time durations [14]. In Fig. 1B, most residues indicate the pattern for the EX2 regime with the pH dependency. However, some of the EX1 regime may be contributed to this reaction especially in the experiments at the higher pH. It is the reason why the value of the final ratio at the longer time seems to be less than one in some cases. Nevertheless, the CLEANEX-PM experiment is a powerful tool to identify the remaining structure in the intrinsically disordered protein.

4.4. Residual structure monitored by CLEANEX-PM

The studies on the alpha-synuclein by the HD exchange and CLEANEX-PM had been conducted by another group [11]. The significant protection had been only observed at the C-terminal regions in alpha-synuclein. In addition, they clearly showed that the protection was effected by the ion-strength, indicating the existence of the electrostatic interaction between the regions. Our results using the fast amide proton exchange by CLEANEX-PM with the fitting procedure showed that the residual structure also exists at the N-terminal part of alpha-synuclein as well as the C-terminal region by collecting the various data points as functions of pH and exchange time durations.

Taking together with the preceding study [11], the protection for the exchange at the C-terminal region is at least partially due to the existence of the negative charge cluster composed of aspartic acid and glutamic acid. The exchange is hindered by the negative charge itself. On the other hand, it is possible that the protection at the C-terminal region is related to the existence of the N-terminal region. Because the N-terminal region is also protected which contains the several positive charge residues, it can be concluded that the electrostatic interaction between the negative and positive charges contributes to the long-range interaction, leading to the formation of the residual structure at the N- and C-terminal regions. The long-range interaction at both ends in the alpha-synuclein is also supported by the PRE [8] and chemical shift [20] experiments.

4.5. Residual structure in alpha-synuclein

The remaining structure of alpha-synuclein at the neutral pH had been studied based on the chemical shift and relaxation studies [5,21]. It was concluded that the rapid fibrillation of the alpha-synuclein was due to the loss of the long-range contact by the comparison studies on the synuclein analogues. The spin-labeling experiment (PRE) is one of the most powerful techniques particularly to figure out the remaining long-range interaction. The long-range interaction between the C-terminal domain and 30–100 region had been indicated at the neutral pH [22]. At lower pH, the PRE studies also showed that the C-terminal region is in more proximity to the NAC region, and probably has lower interactions with the N-terminal region [23]. The protection at the C-terminal region is supposed to be related to the local negative cluster, as well as the long-range interaction as shown above. We are not sure about the reason why the protection is not observed at the NAC region, although the long-range contact exists between the NAC region and the C-terminal region [8,22]. Regarding the long-range contact, the PRE studies give more direct evidence compared to the protection studies.

More recently, the intermolecular interaction of the head-to-tail style and tail-to-tail style had been clearly shown at pH 6 and pH 2.5, respectively [4]. Our data is basically consistent with the data derived from the PRE studies. We demonstrated that the N-terminal (M5–A29) and C-terminal (F94–E137) regions are protected at the neutral pH, and therefore two regions probably interact each other. The CLEANEX-PM experiment is also quite useful, because the advantage is that the data is completely free from any modification of the protein.

The N-terminal end had been shown to be essential to bind to the membrane [24] and apt to be helical structure [25]. It is consistent with our results of the fast exchange (Fig. 4B). The region M5–G7 is highly protected.

4.6. Residual structure in the mutants and amyloid formation

The critical area in the sequence for the amyloid formation of the alpha-synuclein is already known by the biological studies. The responsible area for the amyloid formation including A30P [26], E46K [27], and A53T [28] corresponds to the A30–T64 region, and is almost disordered to the same degree as the NAC region (N65–A90) in our studies. Each mutation might lead to a higher protection at this area to prevent the formation of the stable interacted structure between the N- and C-terminal domains. However, in case of E46K, it was reported that the mutation enhances the contact between the C- and N-terminals to the opposite way [29].

4.7. Differences of the structure between monomer in solution and amyloid

The location of the beta-sheet structure in the amyloid fibril had been shown by the quenched HD exchange [10,30], solid state NMR [10], and the combination of the solution NMR for the unfolded state and solid-state NMR [31]. The beta-sheet regions were composed of L38–K43, V48–N65, V70–Q79, and G86–K97 in the fibril of the alpha-synuclein [30]. Interestingly, all of above-mentioned area is not protected at all in solution in our experiment (Fig. 4B). We have concluded that the beta-sheet area in the fibril takes completely unfolded structure in the soluble monomer. There must be the dramatic structural changes between the physiological soluble condition and amyloid insoluble condition.

Acknowledgements

We thank Drs. Takanori Kigawa and Satoru Watanabe in RIKEN Institute for the technical assistance, and Drs. Yasushi Kawata and Hisashi Yagi in Tottori University for kindly providing the alpha-synuclein plasmid. This work was supported by Grant-in-Aid for Scientific Research (23107726) on Innovative Areas (Molecular Science of Fluctuations toward Biological Functions) and for Scientific Research C (23590049) in Japan. This work was also performed using the Co-operative Research Program of Institute for Protein Research, Osaka University, and RIKEN Institute.

References

[1] Fink, A.L. (2006) The aggregation and fibrillation of alpha-synuclein. Acc. Chem. Res. 39, 628–634.
[2] Spillantini, M.G., Schmidt, M.L., Lee, V.M., Trojanowski, J.Q., Jakes, R. and Goedert, M. (1997) Alpha-synuclein in Lewy bodies. Nature 388, 839–840.
[3] Dauer, W. and Przedborski, S. (2003) Parkinson's disease: mechanisms and models. Neuron 39, 889–909.
[4] Wu, K.P. and Baum, J. (2010) Detection of transient interchain interactions in the intrinsically disordered protein alpha-synuclein by NMR paramagnetic relaxation enhancement. J. Am. Chem. Soc. 132, 5546–5547.
[5] Sung, Y.H. and Eliezer, D. (2007) Residual structure, backbone dynamics, and interactions within the synuclein family. J. Mol. Biol. 372, 689–707.
[6] Sugase, K., Dyson, H.J. and Wright, P.E. (2007) Mechanism of coupled folding and binding of an intrinsically disordered protein. Nature 447, 1021–1025.
[7] Bussell Jr., R. and Eliezer, D. (2001) Residual structure and dynamics in Parkinson's disease-associated mutants of alpha-synuclein. J. Biol. Chem. 276, 45996–46003.
[8] Bertoncini, C.W., Jung, Y.S., Fernandez, C.O., Hoyer, W., Griesinger, C., Jovin, T.M. and Zweckstetter, M. (2005) Release of long-range tertiary interactions potentiates aggregation of natively unstructured alpha-synuclein. Proc. Natl. Acad. Sci. USA 102, 1430–1435.
[9] Giasson, B.I., Murray, I.V., Trojanowski, J.Q. and Lee, V.M. (2001) A hydrophobic stretch of 12 amino acid residues in the middle of alpha-synuclein is essential for filament assembly. J. Biol. Chem. 276, 2380–2386.
[10] Vilar, M., Chou, H.T., Luhrs, T., Maji, S.K., Riek-Loher, D., Verel, R., Manning, G., Stahlberg, H. and Riek, R. (2008) The fold of alpha-synuclein fibrils. Proc. Natl. Acad. Sci. USA 105, 8637–8642.
[11] Croke, R.L., Sallum, C.O., Watson, E., Watt, E.D. and Alexandrescu, A.T. (2008) Hydrogen exchange of monomeric alpha-synuclein shows unfolded structure persists at physiological temperature and is independent of molecular crowding in *Escherichia coli*. Protein Sci. 17, 1434–1445.
[12] Csizmok, V., Felli, I.C., Tompa, P., Banci, L. and Bertini, I. (2008) Structural and dynamic characterization of intrinsically disordered human securin by NMR spectroscopy. J. Am. Chem. Soc. 130, 16873–16879.
[13] Hwang, T.L., van Zijl, P.C. and Mori, S. (1998) Accurate quantitation of water–amide proton exchange rates using the phase-modulated CLEAN chemical EXchange (CLEANEX-PM) approach with a Fast-HSQC (FHSQC) detection scheme. J. Biomol. NMR 11, 221–226.
[14] Hernandez, G., Jenney Jr., F.E., Adams, M.W. and LeMaster, D.M. (2000) Millisecond time scale conformational flexibility in a hyperthermophile protein at ambient temperature. Proc. Natl. Acad. Sci. USA 97, 3166–3170.
[15] Nishimura, C., Lietzow, M.A., Dyson, H.J. and Wright, P.E. (2005) Sequence determinants of a protein folding pathway. J. Mol. Biol. 351, 383–392.
[16] Delaglio, F., Grzesiek, S., Vuister, G.W., Zhu, G., Pfeifer, J. and Bax, A. (1995) NMRPipe: a multidimensional spectral processing system based on UNIX pipes. J. Biomol. NMR 6, 277–293.
[17] Bai, Y., Milne, J.S., Mayne, L. and Englander, S.W. (1993) Primary structure effects on peptide group hydrogen exchange. Proteins 17, 75–86.
[18] Uzawa, T., Nishimura, C., Akiyama, S., Ishimori, K., Takahashi, S., Dyson, H.J. and Wright, P.E. (2008) Hierarchical folding mechanism of apomyoglobin revealed by ultra-fast H/D exchange coupled with 2D NMR. Proc. Natl. Acad. Sci. USA 105, 13859–13864.
[19] Krishna, M.M., Hoang, L., Lin, Y. and Englander, S.W. (2004) Hydrogen exchange methods to study protein folding. Methods 34, 51–64.
[20] Sasakawa, H., Sakata, E., Yamaguchi, Y., Masuda, M., Mori, T., Kurimoto, E., Iguchi, T., Hisanaga, S., Iwatsubo, T., Hasegawa, M. and Kato, K. (2007) Ultra-high field NMR studies of antibody binding and site-specific phosphorylation of alpha-synuclein. Biochem. Biophys. Res. Commun. 363, 795–799.
[21] Wu, K.P., Kim, S., Fela, D.A. and Baum, J. (2008) Characterization of conformational and dynamic properties of natively unfolded human and mouse alpha-synuclein ensembles by NMR: implication for aggregation. J. Mol. Biol. 378, 1104–1115.
[22] Dedmon, M.M., Lindorff-Larsen, K., Christodoulou, J., Vendruscolo, M. and Dobson, C.M. (2005) Mapping long-range interactions in alpha-synuclein using spin-label NMR and ensemble molecular dynamics simulations. J. Am. Chem. Soc. 127, 476–477.
[23] Cho, M.K., Nodet, G., Kim, H.Y., Jensen, M.R., Bernado, P., Fernandez, C.O., Becker, S., Blackledge, M. and Zweckstetter, M. (2009) Structural characterization of alpha-synuclein in an aggregation prone state. Protein Sci. 18, 1840–1846.
[24] Vamvaca, K., Volles, M.J. and Lansbury Jr., P.T. (2009) The first N-terminal amino acids of alpha-synuclein are essential for alpha-helical structure formation in vitro and membrane binding in yeast. J. Mol. Biol. 389, 413–424.
[25] Kang, L., Moriarty, G.M., Woods, L.A., Ashcroft, A.E., Radford, S.E. and Baum, J. (2012) N-terminal acetylation of alpha-synuclein induces increased transient helical propensity and decreased aggregation rates in the intrinsically disordered monomer. Protein Sci. 21, 911–917.
[26] Kruger, R., Kuhn, W., Muller, T., Woitalla, D., Graeber, M., Kosel, S., Przuntek, H., Epplen, J.T., Schols, L. and Riess, O. (1998) Ala30Pro mutation in the gene encoding alpha-synuclein in Parkinson's disease. Nat. Genet. 18, 106–108.
[27] Zarranz, J.J., Alegre, J., Gomez-Esteban, J.C., Lezcano, E., Ros, R., Ampuero, I., Vidal, L., Hoenicka, J., Rodriguez, O., Atares, B., Llorens, V., Gomez Tortosa, E., del Ser, T., Munoz, D.G. and de Yebenes, J.G. (2004) The new mutation, E46K, of alpha-synuclein causes Parkinson and Lewy body dementia. Ann. Neurol. 55, 164–173.
[28] Li, J., Uversky, V.N. and Fink, A.L. (2001) Effect of familial Parkinson's disease point mutations A30P and A53T on the structural properties, aggregation, and fibrillation of human alpha-synuclein. Biochemistry 40, 11604–11613.
[29] Rospigliosi, C.C., McClendon, S., Schmid, A.W., Ramlall, T.F., Barre, P., Lashuel, H.A. and Eliezer, D. (2009) E46K Parkinson's-linked mutation enhances C-terminal-to-N-terminal contacts in alpha-synuclein. J. Mol. Biol. 388, 1022–1032.
[30] Cho, M.K., Kim, H.Y., Fernandez, C.O., Becker, S. and Zweckstetter, M. (2011) Conserved core of amyloid fibrils of wild type and A30P mutant alpha-synuclein. Protein Sci. 20, 387–395.
[31] Kim, H.Y., Heise, H., Fernandez, C.O., Baldus, M. and Zweckstetter, M. (2007) Correlation of amyloid fibril beta-structure with the unfolded state of alpha-synuclein. ChemBioChem 8, 1671–1674.
[32] Croke, R.L., Patil, S.M., Quevreaux, J., Kendall, D.A. and Alexandrescu, A.T. (2011) NMR determination of pK_a values in alpha-synuclein. Protein Sci. 20, 256–269.